

# Microstructure of superconducting ceramics $\text{YBa}_2\text{Cu}_3\text{O}_{7-x}$ sintered with addition of seed grains

M. F. Imayev<sup>1,†</sup>, D. B. Kabirova<sup>1</sup>, R. R. Yakshibayeva<sup>2</sup>

<sup>†</sup>Marcel@imsp.ru

<sup>1</sup>Institute for Metals Superplasticity problems of RAS, S. Khalturina st., 39, Ufa, 450001, Russia

<sup>2</sup>Ufa State Aviation Technical University, K. Marx st., 12, Ufa, 450000, Russia

The growth of seed grains of  $\text{YBa}_2\text{Cu}_3\text{O}_{7-x}$  (Y123) ceramics in fine-grained matrix was studied. For this, two batches of powders were prepared. The first batch consisted only of fine-grained powder with a particle size less than 1  $\mu\text{m}$  and was used to prepare the so-called reference samples. The second batch was a fine-grained powder with addition of 5 wt. % seed grains with sizes 60–80  $\mu\text{m}$ . Powders were pressed and sintered in the temperature range 925–1000°C for 5 h. The effect of sintering temperature on density, grain size, structure of the seed-growth zone were investigated. In samples of both types the highest density is observed after sintering at  $T=925$  °C, and at higher temperatures the density decreases due to a release of oxygen as a result of a partial decomposition of the Y123 phase on grain boundaries. Above  $T\approx 960$ °C the density of the reference samples decreases more strongly than in the samples with seeds. Seeds initiate the growth of anomalously large grains. The strongest growth of large grains occurs at  $T\approx 960$ °C. Above  $T\approx 960$ °C the grain growth is significantly slowed down that is associated with an increase in porosity of the samples. Large grains affect the growth of grains of fine-grained matrix: in the samples with seeds the mean grain size of fine-grained matrix is higher than in the reference samples. A scheme explaining the effect of seed grains on grain growth of fine-grained matrix is proposed.

**Keywords:** superconducting ceramics  $\text{YBa}_2\text{Cu}_3\text{O}_{7-x}$ , sintering, grain growth, seed grains, density.

## 1. Introduction

To obtain a strong texture in such materials as alundum [1–3], mullite [4], and piezoelectrics [5–7] the so-called templated grain growth technique is successfully used. The templates are small (several tens of micrometers) monocrystals of the matrix (main) phase or other substances. The templates from other substances must satisfy the following basic requirements: 1) they must have a crystalline structure similar to the matrix phase and lattice parameters that differ from it by no more than 15%; 2) the matrix phase must be capable to nucleate and grow on a template at high temperatures; 3) the particles of the templates must have an anisotropic shape (plate, disc, whisker) so that they can be oriented under the influence of the applied stresses during shaping of the powder; 4) they must be thermodynamically stable, i.e. do not chemically interact with the matrix or dissolve in it [5]. The templates are added in a small amount (no more than 5%) to the initial powder of the matrix phase, the particle size of which is much smaller than the dimensions of templates. Further, the templates are oriented, as a rule, with uniaxial compression [2] or tape casting [1,3,4,6,7] and subjected to high-temperature annealing. The oriented templates during the recrystallization annealing serve as the nucleation and growth sites of the matrix phase grains, while the matrix grains inherit the texture of the templates. Templated grain

growth is, in fact, a secondary recrystallization on the “seed”. Since the templates are much larger in size than the fine grains of the matrix, they have a significant advantage in the growth rate. When using templates, there is no need to orient all the grains of the matrix, it is enough to create a texture of the templates. Despite the simplicity and the possibility of obtaining a strong texture, the templated grain growth technique has not yet been applied to high-temperature superconducting (HTSC) ceramics. The choice of the material for the templates for HTSC ceramics is complicated by the fact that at high temperatures the latter are chemically active, and superconducting properties are very sensitive to the presence of contaminants. Therefore, it is more reasonable to use single crystals of the matrix phase as templates.

However, before attempting to obtain a texture in a superconductor by adding anisotropic single crystals of the matrix phase to the fine matrix powder, it is necessary to perform the first stage, namely, to study the growth features in a porous fine-grained matrix of artificial recrystallization centers, i.e. large seed grains of matrix phase.

The goal of the present research is to study the growth of large seed grains of  $\text{YBa}_2\text{Cu}_3\text{O}_{7-x}$  (Y123) ceramics in a fine-grained Y123 matrix depending on the sintering temperature and the influence of seed grains on the kinetics of grain growth in a fine-grained matrix.

## 2. Experimental

The initial fine-grained powder Y123 with mean particle size less than 1  $\mu\text{m}$  was prepared by thermolysis of the powder  $\text{Y}_{1.00}\text{Ba}_{1.99}\text{Cu}_{3.10}(\text{NO}_3)_x$  at  $T=850^\circ\text{C}$  for 1 h. A part of the obtained powder was used for preparation of Y123 seed grains. For this purpose, the pressed tablets Y123 were sintered at  $T=1020^\circ\text{C}$  for 1 h. As a result of such sintering, a polycrystal with mean grain size more than 500  $\mu\text{m}$  was obtained. The prepared tablets were crushed into small particles in an agate mortar. The crushed particles were selected by sieves. The particles with the selected size of 60–80  $\mu\text{m}$  were used as seed grains. Next, two weighed portions of powders were prepared. First portion of powder consisted only of a fine-grained powder to be used to prepare the so-called reference samples. The second portion of powder was a fine-grained powder with addition of 5 wt. % of seed grains. Packed powders were pressed into tablets of 5 mm in diameter and 2 mm in height and sintered in air in the temperature range  $T=925\text{--}1000^\circ\text{C}$  for 5 h in an SUOL-0.4.4/12-M2 electric furnace with the accuracy of temperature control within  $\pm 1^\circ\text{C}$ . Metallographic samples were polished with diamond pastes of different granularity and colloidal suspension OP-S (Struers). X-ray diffraction (XRD) data were collected using a DRON-4 diffractometer with filtered  $\text{Cu-K}\alpha$  radiation. Microstructure and chemical composition of the phases were studied with the use of TESCAN VEGA scanning electron microscope. Orientation characteristics of the grains were examined by the EBSD method on a TESCAN MIRRA 3 FEG scanning electron microscope using Oxford CHANNEL program.

Two structural components were distinguished during studying of microstructure: fine-grained matrix (FGM) and large grains grown on seed grains. Since the grains of FGM in the annealed state have plate-like shape, on the basis of measurement of visible length  $l$ , thickness  $h$  the areas of separate grains  $s=l \times h$  were calculated and further the mean values of FGM grains  $S_{FG}$  were defined. The number of grains taken into account was approximately 1000. To determine the mean areas of large grains grown on seed grains  $S_{LG}$ , the areas of separate grains were measured by their image contrast using the Image Pro software. The density of the samples was determined by the geometric method.

## 3. Results

X-ray diffractometry did not reveal any changes in the phase composition up to  $T=990^\circ\text{C}$ . However, after annealing at  $T=1000^\circ\text{C}$  the material becomes a two-phase one: along with Y123 peaks,  $\text{Y}_2\text{BaCuO}_5$  peaks (Y211) are detected. No traces of  $\text{BaCuO}_2$ ,  $\text{CuO}$  and  $\text{CuO}_2$  phases were detected.

Fig. 1 shows the microstructure of the sample with addition of seed grains after sintering at  $T=950^\circ\text{C}$  for 5 h. Two large grains came into the view. It can be seen that during annealing they grew from seed grains. The initial positions of seed grains and their growth zones are marked by dashed and solid lines, respectively. The growth of large grains is accompanied by the capture of pores, in addition,

a large extent of small-angle boundaries marked in red is observed in the growth zone, while high-angle boundaries predominate in the FGM, which are marked in green.

The dependence of the mean grain area of the large grains on the sintering temperature behaves as follows. As the sintering temperature increases to  $T=958^\circ\text{C}$ , the  $S_{LG}$  value increases, and with a further increase in temperature it decreases (Fig. 2). Observation of the shape of the large grains showed the following. At the sintering temperature

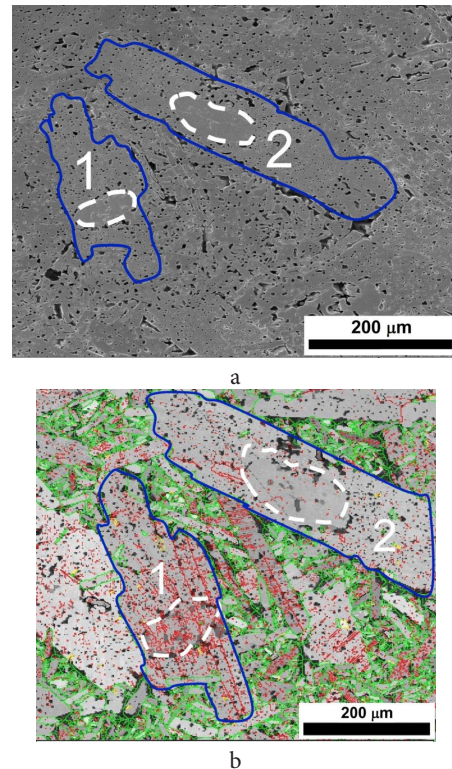


**Fig. 1.** (Color online) Microstructure of Y123 ceramics with addition of seed grains after sintering at  $T=950^\circ\text{C}$  for 5 h: a) in secondary electrons; b) EBSD card in Band Contrast mode. The dashed lines indicate the initial boundaries of seed grains, solid lines — the seed growth zones. The colors of grain boundary misorientation angles: red (1–5°); yellow (5–10°); green (10–90°).

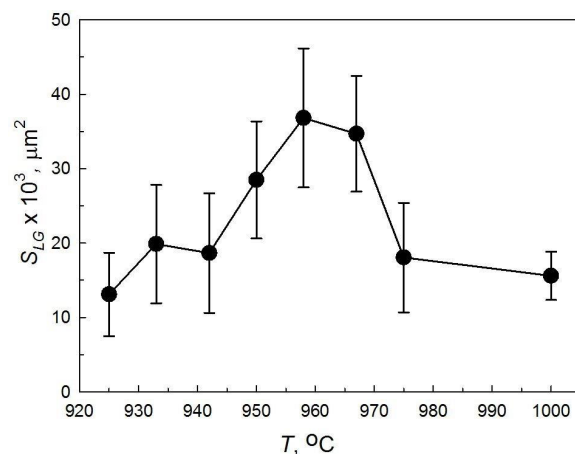


**Fig. 2.** Dependence of area of large grains  $S_{LG}$  growing on seed grains on sintering temperature.

$T=933^{\circ}\text{C}$  the seed growth zones begin to acquire a plate-like shape. At  $T=942^{\circ}\text{C}$  the plate-like shape of the grains becomes more pronounced. After sintering at  $950^{\circ}\text{C}$  or higher all large grains have a plate-like shape and impinge with each other.

Presented in Fig. 3 are the dependencies of the main grain area of FGM for samples with seed grains and reference samples. It can be seen that both dependences pass through a maximum at  $T=950^{\circ}\text{C}$ . At the same time, the grain area FGM in samples with seed grains is markedly higher than in reference samples. The dependences of the standard deviation of grain area distribution  $\sigma(s)$  of the FGM on the sintering temperature behave similarly. Both dependences pass through a maximum at  $T=950^{\circ}\text{C}$ , and in the temperature range where the grain growth is observed ( $925-975^{\circ}\text{C}$ ) the width of the distribution curve for samples with seed grains is wider than for the reference samples (Fig. 3).

In both types of samples the highest density is  $\rho \approx 5.6 \text{ g/cm}^3$  (88% of the theoretical density) after sintering at  $T=925^{\circ}\text{C}$ , and after sintering at higher temperatures it decreases (Fig. 4). As the sintering temperature increases from  $T=925^{\circ}\text{C}$  to  $958^{\circ}\text{C}$ , the densities of both types of samples decrease, but remain approximately the same. After sintering at temperatures above  $T=958^{\circ}\text{C}$  the density of reference samples decreases more strongly than in samples with seed grains.

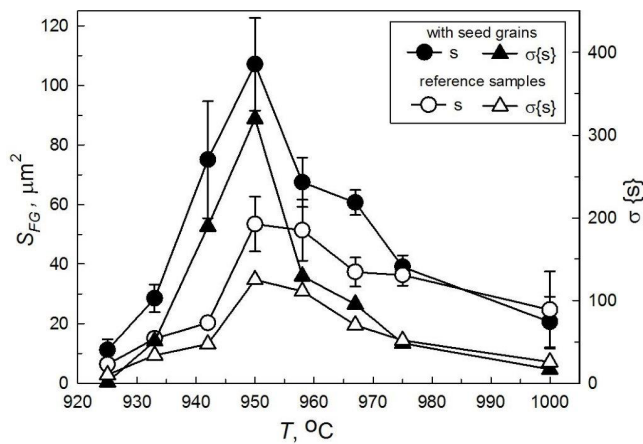


Fig. 3. Dependences of mean grain area  $S_{FG}$  and standard deviation of grain area distribution  $\sigma(s)$  of fine-grained matrix on sintering temperature for samples with seed grains and reference samples.

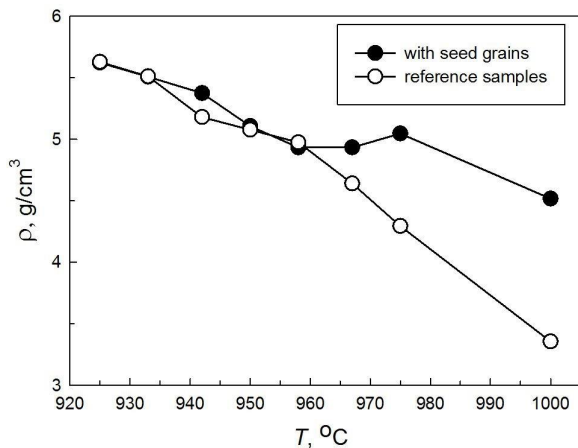


Fig. 4. Dependence of sample density on sintering temperature.

### 4. Discussion

Before proceeding to discuss the results obtained, it should be noted that the Y123 phase is a strict line compound with an area of solid state solubility by cations less than 0.5 wt.% [8]. Therefore, small local deviations from stoichiometry can result in partial melting due to eutectic  $e_1$ ,  $e_2$  and peritectic  $p_1$  reactions at temperatures well below the incongruent melting temperature  $m_1$  (Table 1) [9]. Grain boundaries are the places where a deviation from stoichiometry often takes place.

Table 1. Invariant reactions in the Y-Ba-Cu-O system observed in air [9]

Инвар. точка	Реакция	$T, ^{\circ}\text{C}$
$e_1$	$\text{Y123} + \text{BaCuO}_2 + \text{CuO} \rightarrow \text{L}(e_1) + \text{O}_2$	898
$e_2$	$\text{BaCuO}_2 + \text{CuO} \rightarrow \text{L}(e_2) + \text{O}_2$	902
$p_1$	$\text{Y123} + \text{CuO} \rightarrow \text{Y}_2\text{BaCuO}_5 + \text{L}(p_1) + \text{O}_2$	933
$m_1$	$\text{Y123} \rightarrow \text{Y}_2\text{BaCuO}_5 + \text{L}(m_1) + \text{O}_2$	1015

First, we discuss the reason for the decrease in the density of ceramics with increasing sintering temperature. This will allow understanding the peculiarities of change in the grain size, because the processes of pore healing and grain growth are interrelated [10, 11]. The decrease in density correlates with the termination of the peritectic melting reaction  $p_1$  at the grain boundaries, which occurs in the temperature range  $930-950^{\circ}\text{C}$  [9]. It would seem that an increase in the amount of liquid resulting from the reaction  $p_1$  should lead to an additional compaction of the ceramics, however, the density decreases. This is due to the fact that along with the liquid and the solid phase Y211, oxygen is released. Apparently, it is precisely that the oxygen release leads to an increase in porosity. As a result of the release of oxygen during the reaction  $p_1$ , the weight loss compared to the initial mass is about 0.07% [12]. As the sintering temperature increases in the temperature range between points  $p_1$  and  $m_1$ , the amount of oxygen released continues to increase due to the increase in the amount of liquid and decomposition of the Y123 phase. At the same time, the composition of the liquid varies along the peritectic line  $p_1-m_1$  and enriches with barium and copper. Above  $T \approx 985^{\circ}\text{C}$  the release of oxygen is further increased because of the onset of incongruent melting of Y123 on the grain boundaries. In this case the mass loss is about 0.7% [12].

According to the modern concepts, filling a pore with liquid is a necessary condition for healing it during liquid-phase sintering. The pore filled with liquid is capable to be healed by directional growth of adjacent grains [10]. In the case of ceramics Y123 at sintering temperatures above  $T=950^{\circ}\text{C}$  most of the pores are apparently filled with gaseous oxygen, and their healing process is strongly inhibited, which ultimately causes a low sample density.

After sintering above  $T=950^{\circ}\text{C}$  the density of the reference samples decreases more rapidly than in samples with seed grains. This is explained by the fact that the total area of the grain boundaries in the reference samples is higher, especially

after sintering at temperatures above  $T=950^{\circ}\text{C}$ , when the majority of large grains grown on seed grains have impinged with each other. And, since the decomposition of the Y123 phase and the release of oxygen occur mainly at the grain boundaries, the higher the total grain boundary area, the more oxygen is released and the higher the residual porosity.

The decrease in the main grain size of Y123 at sintering above  $T=950^{\circ}\text{C}$  can be explained by two factors: 1) an increase in the porosity and 2) the precipitation of particles of the Y211 phase. The strongest suppression of the grain growth is observed near  $T=1000^{\circ}\text{C}$  that is due to the release of additional amounts of oxygen and particles Y211 as a result of the reaction  $m_1$  [13].

Let us now discuss the fact of a more intensive growth of FGM in samples with addition of seed grains than in comparison to the reference samples. It is known that the grain growth in Y123 ceramics is an Ostwald ripening, and the Y123 grains grow due to the diffusion of atoms between grains through a liquid intergranular film [14]. The driving force of this process is the minimization of the free surface energy of the contacting grains. For a system of grains distributed in a liquid media, the driving force  $\Delta g_r$  for grain growth with effective radius  $r$  and average surface energy  $\sigma$  is [15]:

$$\Delta g_c = 2\sigma V_m \left( \frac{1}{\bar{r}} - \frac{1}{r} \right), \quad (1)$$

where  $V_m$  — molar volume of solid phase and  $\bar{r}$  — critical radius of grains neither growing nor shrinking, which is the time variant. Thus, when annealing, grains with  $r > \bar{r}$  will grow, and grains with  $r < \bar{r}$  will dissolve.

Numerous experimental results and modeling data indicate that the initial grain size distribution affects the rate of microstructure enlargement. Thus, initially wide grain size distributions are coarsened faster than narrow ones [16–19]. Therefore, the fact that in Y123 samples with addition of seed grains the width of the grain size distribution of FGM is wider than that of the reference samples and the mean grain size grows faster indicates that the large grains grown on the seed grains influence the grain size distribution of FGM and, accordingly, the growth rate of FGM. This assumption is supported by modeling data showing that the microstructure that has an initially long tail of distribution corresponding to large grains is most rapidly coarsened [20]. Another factor is possible that promotes the acceleration of the growth of FGM in samples with addition of a seed grains. Large grains in the course of their growth displace liquid and increase its concentration in the FGM. As a result, complete wetting of the grains is achieved, and the growth rate of the FGM increases.

Fig. 5 shows a one-dimensional grain growth scheme explaining the observed effect of the influence of seed grains on the width of the grain size distribution and main grain size of FGM. Grains are represented by rectangles, the long sides of which are located along a horizontal line. First consider a reference sample, in which there are no seed grains. The grain size distribution is narrow, therefore grains are represented by rectangles with approximately the same dimensions (Fig. 5a). In such a microstructure, the grains do not have much advantage in size before the neighbors, so the rate of grain growth is low. When adding seed grains the equilibrium

of system is disrupted (Fig. 5b–d). The large grain grown on the seed grain due to its strong dimensional advantage begins to rapidly absorb the grain 1. Grain 2, having gained an advantage over grain 1, also begins to absorb it. The grown grain 2 becomes larger than grain 3, so it begins to absorb it as well. The reducing size of grain 3 leads to the fact that it, in turn, begins to be absorbed by grain 4 (Fig. 5c). As a result, at a certain stage, grains 1 and 3 are absorbed by larger neighboring grains (Fig. 5d).

Thus, the introduction of a small number of seed grains into initial fine powder leads to broadening of the grain size distribution and acceleration of grain growth in the FGM. This must be taken into account when carrying out the texturing of the material, since the growth of FGM grains will be accompanied by a decrease in the driving force of growth of the templates and slowing their growth, which may lead to the formation of an incompletely recrystallized microstructure.

### 5. Conclusions

1. In the samples with seed grains and reference samples the highest density ( $5.6 \text{ g/cm}^3$ ) is observed after sintering at  $T=925^{\circ}\text{C}$  and it decreases at higher temperatures. With an increase in the sintering temperature to  $T=958^{\circ}\text{C}$ , the densities of the samples of both types are approximately the same and decrease to  $5 \text{ g/cm}^3$ , and at temperatures above  $T=958^{\circ}\text{C}$  the density of the reference samples decreases more strongly than in the samples with seed grains. The decrease in density is caused by the release of oxygen, which accumulates in the pores and prevents their healing.

2. Seed grains initiate the growth of large grains. The growth of the large grains of Y123 begins at  $T \sim 925^{\circ}\text{C}$ . At  $T=933^{\circ}\text{C}$  the grains start to acquire a plate-like shape, and at  $T=942^{\circ}\text{C}$  almost all large grains have a plate-like shape. The strongest growth of grains occurs at  $T=958^{\circ}\text{C}$ . At temperatures above  $958^{\circ}\text{C}$  the grain growth is significantly slowed down, which is associated with an increase in the porosity of the samples.

3. Large grains growing on seed grains affect the growth of grains of a fine-grained matrix. In samples with the addition of seed grains the average grain size of the fine-grained matrix is higher than in the reference samples.

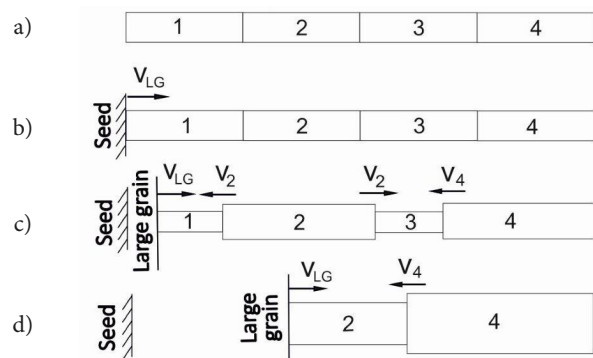


**Fig. 5.** One-dimensional model of grain growth in ceramics Y123 with addition of seed grains. Numbers 1–4 indicate grains of a fine-grained matrix;  $V_{LG}$  and  $V_1 - V_4$  designate the directions of growth of large grain and grains 1–4, respectively.

## References

1. M.M. Seabaugh, I.H. Kerscht, G.L. Messing. *J. Am. Ceram. Soc.* 80 (5), 1181 (1997).
2. E. Suvaci, M.M. Seabaugh, G.L. Messing. *J. Eur. Ceram. Soc.* 19, 2465 (1999).
3. R.J. Pavlacka, G.L. Messing. *J. Eur. Ceram. Soc.* 30, 2917 (2010). DOI: 10.1016/j.jeurceramsoc.2010.02.009.
4. E. Gönenli, G.L. Messing. *J. Eur. Ceram. Soc.* 21, 2495 (2001).
5. Messing G.L., Trolier-McKinstry S., Sabolsky E.M., Duran C., Kwon S., Brahmaroutu B., Park P. *Critical Reviews in Solid State and Materials Sciences* 29, 45 (2004). DOI: 10.1080/10408430490490905
6. S. Kwon, E.M. Sabolsky, G.L. Messing, S. Trolier-McKinstry. *J. Am. Ceram. Soc.* 88 (2), 312 (2005). DOI: 10.1111/j.1551-2916.2005.00057.x
7. Y. Chang, Y. Sun, J. Wu, X. Wang, S. Zhang, B. Yang, G.L. Messing, W. Cao. *J. Eur. Ceram. Soc.* 36, 1973 (2016). DOI: 10.1016/j.jeurceramsoc.2016.02.030
8. Scheel H.J., Licci F. *Thermochim. Acta.* 174, 115 (1990).
9. Aselage T., Keefer K. *J. Mater. Res.* 3 (6), 1279 (1988).
10. Suk-Joong L. Kang. *Sintering: densification, grain growth and microstructure.* Elsevier Butterworth-Heinemann. (2005) 266 p.
11. Imayev M.F., Kabirova D.B., Sagitov R.I., Churbaeva H.A. *J. Eur. Ceram. Soc.* 32, 1261 (2012). DOI: 10.1016/j.jeurceramsoc.2011.10.046
12. E.R. Benavidez, C. J. R. Gonzalez Oliver. *J. Mater. Sci.* 40, 3749 (2005).
13. Imayev M.F., Kabirova D.B., Churbaeva H.A., Salishchev G.A. *Proc. of the First Joint International Conference On Recrystallization and Grain Growth (Rex&GG 2001).* Aachen, Germany. (2001) p. 339–344.
14. Imayev M.F., Kazakova D.B., Gavro A.N., Trukhan A.P. *Physica C.* 329, 75 (2000).
15. Y.-I. Jung, D.Y. Yoon, S.-J.L. Kang. *J. Mater. Res.* 24 (9), 2949 (2009). DOI: 10.1557/JMR.2009.0356
16. Z. Fang, B.R. Patterson, M.E. Turner. *Acta Metall.* 40 (4) 713 (1992).
17. J.-M. Ting, R. Y. Lin. *J. Mater. Sci.* 30, 2382 (1995).
18. W.E. Benson, J.A. Wert. *Acta Mater.* 46 (15) 5323 (1998).
19. C. Wang, G. Liu, X. Qin. *J. Mater. Sci. Lett.* 22, 473 (2003).
20. J. Li, C. Guo, Y. Ma, Z. Wang, J. Wang. *Acta Mater.* 90, 10 (2015). DOI: 10.1016/j.actamat.2015.02.030